

# PROCEEDINGS OF SPIE

[SPIDigitalLibrary.org/conference-proceedings-of-spie](https://spiedigitallibrary.org/conference-proceedings-of-spie)

## Nonrigid registration of 3D longitudinal optical coherence tomography volumes with choroidal neovascularization

Qiangding Wei, Fei Shi, Weifang Zhu, Dehui Xiang, Haoyu Chen, et al.

Qiangding Wei, Fei Shi, Weifang Zhu, Dehui Xiang, Haoyu Chen, Xinjian Chen, "Nonrigid registration of 3D longitudinal optical coherence tomography volumes with choroidal neovascularization," Proc. SPIE 10133, Medical Imaging 2017: Image Processing, 101330X (24 February 2017); doi: 10.1117/12.2253999

**SPIE.**

Event: SPIE Medical Imaging, 2017, Orlando, Florida, United States

# Nonrigid Registration of 3D Longitudinal Optical Coherence Tomography Volumes with Choroidal Neovascularization

*Qiangding Wei<sup>1</sup>, Fei Shi<sup>1</sup>, Weifang Zhu<sup>1</sup>, Dehui Xiang<sup>1</sup>, Haoyu Chen<sup>2</sup>, Xinjian Chen<sup>\*1</sup>*

<sup>1</sup>School of Electronics and Information Engineering, Soochow University, Suzhou, China

<sup>2</sup>Joint Shantou International Eye Center, Shantou University and the Chinese University of Hong Kong, Shantou, China

## ABSTRACT

In this paper, we propose a 3D registration method for retinal optical coherence tomography (OCT) volumes. The proposed method consists of five main steps: First, a projection image of the 3D OCT scan is created. Second, the vessel enhancement filter is applied on the projection image to detect vessel shadow. Third, landmark points are extracted based on both vessel positions and layer information. Fourth, the coherent point drift method is used to align retinal OCT volumes. Finally, a nonrigid B-spline-based registration method is applied to find the optimal transform to match the data. We applied this registration method on 15 3D OCT scans of patients with Choroidal Neovascularization (CNV). The Dice coefficients (DSC) between layers are greatly improved after applying the nonrigid registration.

**Keywords:** coherent point drift, optical coherence tomography, 3D nonrigid registration

## 1 Introduction

Optical coherence tomography has become an important modality in ophthalmic imaging since its introduction in 1991. It has enabled acquisition of high resolution, 3D cross-sectional volumetric image of retina. It assists the ophthalmologists to observe the retinal morphology more clearly and to diagnose more accurately. The 3D OCT is very useful for detecting retinal pathological changes in serious eye diseases such as age-related macular degeneration (AMD) with choroidal neovascularization (CNV). CNV is a kind of pathology that grows from the choroid and is one important cause of visual disability. So far, its pathogenetic mechanism is not clear. Tracking the change of pathological regions is important during the treatment of CNV. Fig.1 shows unprocessed B-scans from three longitudinal OCT volumes of one CNV patient receiving monthly anti-VEGF injection. To track these disease changes over time, registration of 3D OCT scans of the same eye is important. Through 3D OCT registration, the change of the disease can be analyzed quantitatively, which can be used to assess the effectiveness of the treatment and to guide further treatment planning.

Image registration techniques in computer vision, medical image processing, and other fields have a wide range of applications. Especially in medical image processing area, it is a vital tool to enable more precise, quantitative comparison of disease states. Registration of point sets is a key component in image registration. The goal of point set registration is to assign correspondences between two sets of points and/or recover the transformation that maps one point set to the other. However, accurate and efficient image registration is difficult. Several approaches for 3D OCT scans registration have been proposed in [1, 2]. The method in [1] only used translation along X, Y and Z axes to align the volumes. In [2], it first used the iterative closest point (ICP) to register the XY domain, and then used the graph-based method to translate the individual A-scans along the depth axis. These are not fully 3D registration methods.

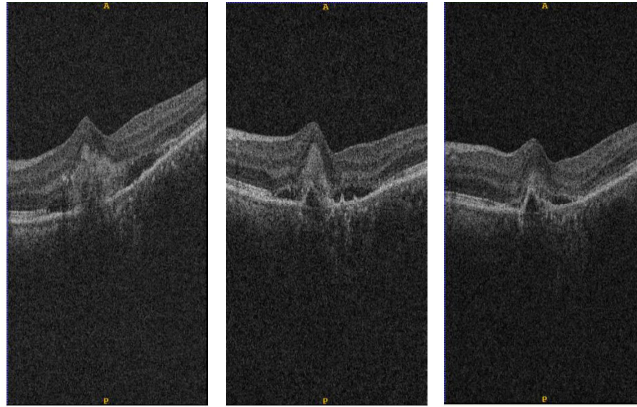


Fig. 1 (a), (b), (c) unprocessed B-scans from three longitudinal OCT volumes of one CNV patient receiving monthly anti-VEGF injection.

A fully 3D registration method was proposed in [3], but it only registered the vessel point sets and the registration result for the whole 3D volume was not evaluated. Other works in this area focused on OCT to fundus registration [4, 5], where healthy cases were used. In this work, we propose a completely 3D registration method for retinal optical coherence tomography volumes with choroidal neovascularization (CNV), and we use both vessel point sets and part of the surface points as landmarks. The registration results for the OCT volumes are quantitatively evaluated.

## 2 Methodology

The proposed method consists of five main steps. First, pre-processing is applied to create a projection image. Second, the vessel enhancement filter is used to detect vessel shadows. Third, three dimensional landmarks are obtained. Fourth, OCT volumes are aligned based on coherent point drift (CPD) method. Finally, a nonrigid registration method is applied. An overview of the proposed method is shown in Fig. 2, More details are given as follows:

### 2.1. Pre-processing

#### 2.1.1. Denoising

Speckle noise is the main quality degrading factor in OCT scans. The denoising method applied to OCT image should be efficient for speckle noise suppression. So a 3D curvature anisotropic diffusion filter [6] is adopted.

#### 2.1.2. Surface segmentation

Then, a 3-D multi-scale graph search method is applied for abnormal retinal layer segmentation [7]. Five surfaces segmenting retina layers are found. As shown in Fig. 3(a), surface1 and 2 are upper and lower boundaries of nerve fiber layer (NFL), surface3 is lower boundary of inner nuclear layer (INL), surface4 is the boundary of inner and outer retina, surface5 is the Bruch's membrane (BM). Mean gray value of all the outer retina layers between surface4 and surface5 is calculated to obtain the projection image, which is then interpolated to form an isotropic image ( $512 \times 512$  pixels) (Fig.3 (b)).

#### 2.1.3. Pathology Removal

For CNV patients, sub-retinal fluid may cause non-vessel shadows. This is with similar intensity to blood vessels. However, vessels are generally long, thin connected regions. Therefore, shape characteristics and position information

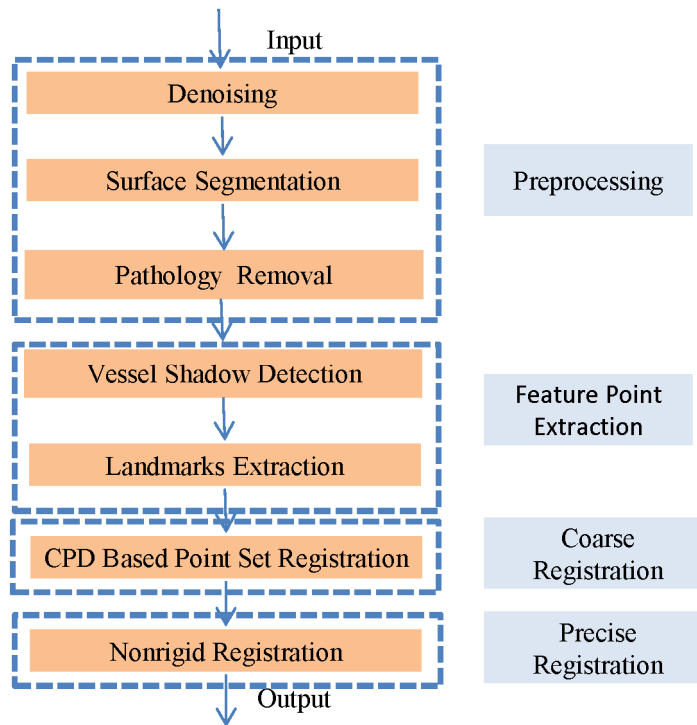


Fig.2 The flowchart of the proposed method

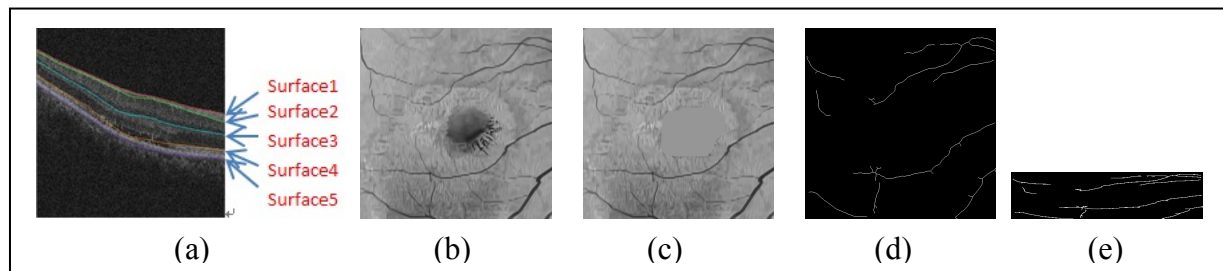


Fig. 3 (a) layer segmentation image, (b) projection image, (c) (b) with non-vessel shadows removed, (d) segmented vessel shadows with a single pixel remains, (e) down-sampled image of (d).

are used to distinguish these two kinds of shadows. For each projection image, randomly selected intensities from the object boundary are used to fill the non-vessel shadows (Fig. 3(c)).

## 2.2. Vessel Shadow Detection

We apply the vessel enhancement filter [8] to the processed projection image (Fig. 3(c)) to detect tubular structures and suppress remaining noise and background.

Then the mathematical morphology method was applied to find the skeleton of vessels (Fig. 3(d)). It ensures only a single pixel remains along the structure while preventing the structure from breaking apart.

Finally, it is down-sampled to the original size ( $512 \times 128$  pixels) (Fig. 3(e)). Based on the two-dimensional coordinates of the blood vessels, the corresponding coordinates in 3D can be found.

### 2.3. Landmarks extraction

For 3D registration, landmarks are determined by back-projection of the 2D vessel points in the 3D volume. Typically, in OCT data, vessel appear as hyper-reflective regions followed by the shadowing of structures beneath them due to light adsorption by blood [9]. Therefore, the points with the maximum intensity between surface2 and surface3 are found as the vessel points in 3D OCT.

To add more constraints to the 3D registration, the projection of 2D vessel points on the surface1 (ILM) and surface5 (BM) are also used as landmarks. So, both vessel point sets and part of layer information are used in landmark extraction. These landmark points are used as the point set in the CPD registration method.

### 2.4. Point Set Registration with CPD

The CPD algorithm [10] considers the alignment of two point sets as a probability density estimation problem, where one point set represents the Gaussian mixture model (GMM) centroids and the other one represents the data points. Myronenko et al. [10] added a weighted uniform distribution to the mixture model, and make it account for noise and outliers. The maximum of the GMM posterior probability for a given data point can define the correspondence. In this paper, we apply this method with the affine transform model to obtain the correspondence of the two sets of extracted landmarks, which leads to a coarse registration result.

The affine registration is defined as  $T(y_m; R, t, s) = By_m + t$ , where  $B_{D \times D}$  is an affine transformation matrix, and  $t_{D \times 1}$  is the translation vector. The objective function takes the form:

$$Q(B, t, \sigma^2) = \frac{1}{2\sigma^2} \sum_{m,n=1}^{M,N} P^{old}(m | x_n) \|x_n - (By_m + t)\|^2 + \frac{N_p D}{2} \log \sigma^2 \quad (1)$$

where  $D$  denotes the dimension of the point sets,  $N_p = \sum_{n=1}^N \sum_{m=1}^M P^{old}(m | x_n) \leq N$  and

$$P^{old}(m | x_n) = \frac{\exp\left(-\frac{1}{2} \left\| \frac{x_n - T(y_m, \theta^{old})}{\sigma^{old}} \right\|^2\right)}{\sum_{k=1}^M \exp\left(-\frac{1}{2} \left\| \frac{x_n - T(y_k, \theta^{old})}{\sigma^{old}} \right\|^2\right) + (2\pi\sigma^2)^{D/2} \frac{\omega}{1-\omega} \frac{M}{N}} \quad (2)$$

CPD algorithm finds parameters  $\theta$  and  $\sigma^2$  by Expectation Maximization(EM) iteration. E-step: to estimate the initial parameters, and use the Bayes' theorem to compute a posterior probability distributions of mixture components. M-step: to update parameters by minimizing the objective function in (1). Matrix  $B_{D \times D}$  and  $t_{D \times 1}$  are then generated from

the registered vessel points and part of the surface points. Then, based on the  $B_{D \times D}$  and  $t_{D \times 1}$ , the moving image can be registered to the fixed image, we have obtained the final registered OCT images.

## 2.5. Nonrigid registration

Because of the deformation of retina caused by growth or shrinkage of pathological regions, the correspondence between OCT images may not be fully described by the affine registration. Therefore the nonrigid registration B-spline transform [11] is further applied on the initial registration results obtained by CPD. Control points and spline functions are used to describe the nonlinear geometric transform. The B-spline transform is modeled as a weighted sum of B-spline basis functions, placed on a uniform control point grid. When these control points have space displacement, the spline functions are bent so that image space around the control points also bends, which produces different degrees of distortion.

In the three-dimensional space, we denote the domain of the image volume as  $\Omega = \{(x, y, z) | 0 \leq x < X, 0 \leq y < Y, 0 \leq z < Z\}$ , the free-form deformation based on B-spline function can be described as a tensor product of three dimensional B-spline functions:

$$T(x, y, z) = \sum_{l=0, m=0, n=0}^{3,3,3} B_{l,3}(u)B_{m,3}(v)B_{n,3}(w) \times P_{i+l, j+m, k+n} \quad (3)$$

where  $B_i(u)$  is the basis function of the B-spline,

$$B_{0,3}(u) = \frac{(1-u)^3}{6} \quad (4)$$

$$B_{1,3}(u) = \frac{3u^3 - 6u^2 + 4}{6} \quad (5)$$

$$B_{2,3}(u) = \frac{-3u^3 + 3u^2 + 3u + 1}{6} \quad (6)$$

$$B_{3,3}(u) = \frac{u^3}{6} \quad (7)$$

A B-spline free-form deformation represents a nonrigid transformation by manipulating a mesh of control points overlaid on the image domain  $\Omega$ . The control points act as the parameters of the B-spline free-form deformation. This method transforms the registration problem into the three b-spline local control problem. A nonrigid transformation  $T$  of any voxel  $(x, y, z)$  is calculated by its surrounding neighborhood of control points in (3).

### 3 Experimental Results

#### 3.1 Subject Data

The proposed method was tested on longitudinal 3D OCT scans of five patients with Choroidal Neovascularization (CNV), who were receiving anti-VEGF treatment. Fifteen 3D CNV OCT data obtained from Zeiss with a size of  $512 \times 128 \times 1024$  voxels ( $6\text{mm} \times 6\text{mm} \times 2\text{mm}$ ) were used in this study. Each CNV patient has about 5 points in time. In this study, time point 1 is used as the fixed image and the other time points are used as the moving image.






#### 3.2 Assessment of registration Performance

To quantify the registration performance, the dice similarity coefficient (DSC) of retinal layers between fixed and registered OCT images was used to evaluate the accuracy of the results, where the layers are labeled manually. This was calculated for each layer  $k$  using,

$$d_k = \frac{2|T_K \cap S_k|}{|T_K| + |S_k|} \quad (8)$$

Where  $T_K$  and  $S_k$  are the set of voxels labeled as layer  $k$  in the fixed image, and the registered image, respectively. A

Dice coefficient of 1.0 corresponds to complete overlap between  $T_K$  and  $S_k$ , while a score of 0.0 means no overlap between the two. A list of the segmented layers is shown in Fig. 4. Table 1 shows the DSC for five retinal layers. Fig.5 shows some of fixed images, moving images and the registered images.

Name	Abbr.	
Retinal nerve fiber layer	RNFL	
Ganglion cell layer and Inner plexiform layer	GCL+ IPL	
Inner nuclear layer and Outer plexiform layer	INL+OPL	
Outer nuclear layer	ONL	
Inner segment/Outer segment and Retinal pigment epithelium	IS/OS+RPE	

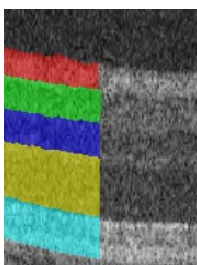


Fig.4, List and partial examples of layers manually segmented in the test data.

Table 1 DSC between the fixed image and the registered image (averaged over 12 registrations) .

	Layers					Mean
	RNFL	GCL+IPL	INL+OPL	ONL	IS/OS+RPE	
CPD	0. 27	0. 31	0. 30	0. 39	0. 35	0.32
CPD+nonrigid	0. 69	0. 75	0. 70	0. 72	0. 80	0.73

### 4 Discussion and Conclusion

In this paper, we proposed a 3D two-stage registration method of 3D retinal OCT volumes, which combines the feature-based method with the intensity-based registration. In the feature-based method, both vessel and layer information are used to obtain landmarks. The proposed method was tested on 12 pairs of 3D OCT scans of patients with CNV. The results showed the effectiveness of the proposed method.

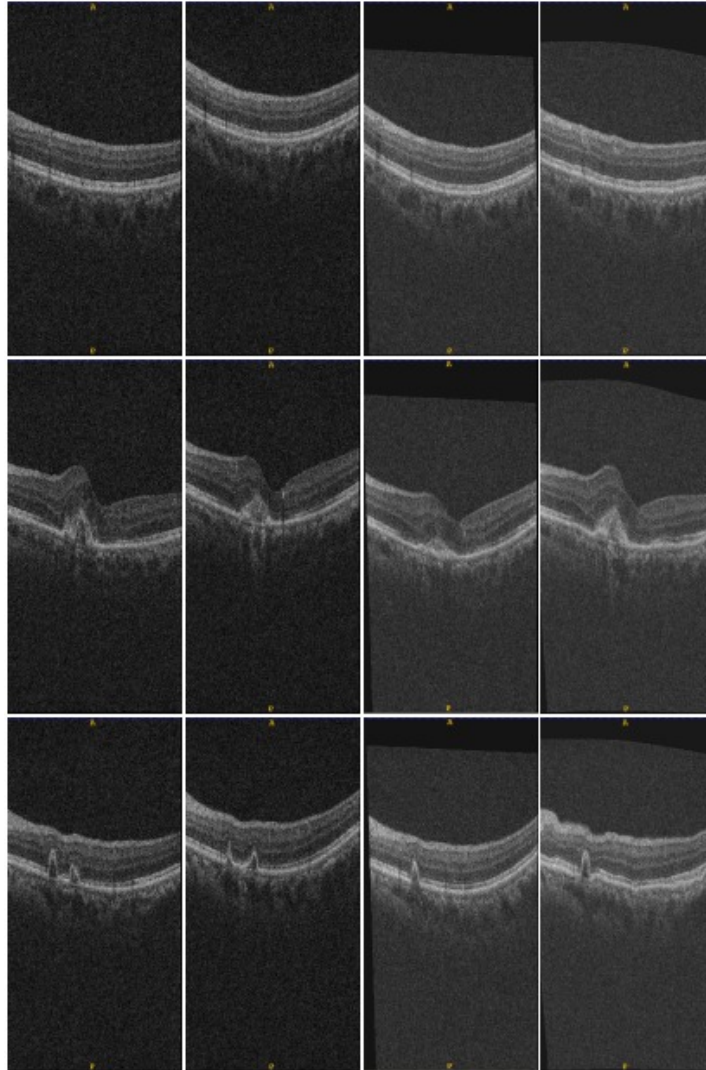


Fig.5, The first column are fixed images, the second column are moving images, the third column are registered images based on CPD. the forth column are registered images based on CPD and B-spline.

**ACKNOWLEDGEMENTS**

This work has been supported by the National Basic Research Program of China (973 Program) under Grant No. 2014CB748600, the National Natural Science Foundation of China (NSFC) under Grants No. 61401294, 81401472, 61401293, 81371629, 61622114, and the Natural Science Foundation of the Jiangsu Province under Grant No. BK20140052, and graduate student innovation Program under Grant KYZZ16\_0084.

**REFERENCES**

[1] M. Niemeijer, M. K. Garvin, K. Lee, B. van Ginneken, M. D. Abr’ amoff, and M. Sonka, “Registration of 3d spectral oct volumes using 3d sift feature point matching,” *Medical Imaging 2009: Image Processing* 7259(1), p. 72591I, SPIE, 2009.



- [2] Niemeijer, M., Lee, K., Garvin, M.K., Abramoff, M.D., Sonka, M.: Registration of 3d spectral oct volumes combining ICP with a graph based approach. In: SPIE Medical Imaging. Volume 8314. (February 2012)
- [3] Jing Wu, Bianca S. Gerendas, Sebastian M. Waldstein, Georg Langs, Christian Simader, and Ursula SchmidtErfurth, "Stable Registration of Pathological 3D SD- OCT Scans using Retinal Vessels", Proceedings of MICCAI Ophthalmic Medical Image Analysis Workshop'14, (2014)
- [4] Kolar, R., Tasevsky, P.: Registration of 3D Retinal Optical Coherence Tomography Data and 2D Fundus Images. BIR 6204 (2010) 72–82
- [5] Golabbakhsh, M., Rabbani, H.: Vessel-based registration of fundus and optical coherence tomography projection images of retina using a quadratic registration model. IET Image Processing 7 (2013) 768–76
- [6] Zhuli Sun, Haoyu Chen, Fei Shi, Lirong Wang, Weifang Zhu, Dehui Xiang, Chenglin Yan, Liang Li, Xinjian Chen\*. An automated framework for 3D serous pigment epithelium detachment segmentation in SD-OCT images. Scientific reports,6, Article number:21739,doi:10.1038/srep21739,2016.
- [7] Fei Shi, Xinjian Chen\*, Heming Zhao, Weifang Zhu, Dehui Xiang, Enting Gao, Milan Sonka and Haoyu Chen , Automated 3-D Retinal Layer Segmentation of Macular Optical Coherence Tomography Images with Serous Pigment Epithelial Detachments ,IEEE TRANSACTIONS ON MEDICAL IMAGING ,Vol. 34, No.2, pp.441 - 452, 2015.
- [8] Frangi, A., Niessen, W.J., Vincken, K.L., Viergever, M.A.: Multiscale vessel enhancement filtering. MICCAI 1496 (1998) 130–37
- [9] Drexler, W., Fujimoto, J.G.: Optical Coherence Tomography: Technology And Applications Springer(2008)
- [10] Myronenko, A., Song, X.: Point Set Registration: Coherent Point Drift. PAMI 32(2010) 2262–2275
- [11] D. Rueckert, L. I. Sonoda, and C. Hayes et al., "Nonrigid registration using free-form deformations: Application to breast MR images," IEEE Trans. Med. Imag., vol. 18, no. 8, pp. 712–721, Aug. 1999.